Fracture Mechanics of Concrete Structures,
Proceedings FRAMCOS-2, edited by Folker H. Wittmann,
AEDIFICATIO Publishers, D-79104 Freiburg (1995)

FAILURE OF CONCRETE WITH OBLIQUE WEAK LAYER

H. Wang and X.Z. Hu
Department of Mechanical and Materials Engineering
University of Western Australia,
Perth, Australia

Abstract

Compressive failure of brittle heterogeneous materials such as rock and concrete is strongly influenced by weak planes or layers contained in these materials. Those weak layers can be due to either the damage accumulation through localised micro-cracking or the inherent defects in the heterogeneous structures.

To study the influence of the weak layers on compressive failure of concrete-like materials, mortar specimens with controlled weak layers have been tested. The weak layer in a specimen has pre-determined thickness and angle, and its strength is controlled by the water/cement and sand/cement ratios. Specimens with weak layers of 5, 10 and 15 mm thick and angles from 0° to 55° have been tested. The shear strain-softening of the weak layer material has been deducted from stable load-displacement curves. Creep and stress relaxation can also be studied and monitored because of the pre-determined damage zone - the weak layer.

1 Introduction

Tensile fracture of concrete has been successfully modelled by cohesive cracks which are controlled by the well-known strain-softening behaviour measured from a plain tensile specimen after the maximum

load has been reached (Hillerborg et al 1976). The significance of the tensile strain-softening behaviour is reflected by the abundant publications on its measurement and application in concrete fracture analysis.

While the models and testing techniques are being refined for the Mode-I fracture of concrete, considerable efforts have also been directed to the Mode-II shear failure and the mixed-I and -II fracture (e.g. Luong 1989, Barr et al 1989, Jenq and Shah 1989). However, it seems that a well-accepted model as well as a well-defined testing technique, like the tensile strain-softening behaviour for the Mode-I fracture, is yet to be further verified.

The standard compressive test with plain un-notched concrete samples has been established for many years. The test is easy to perform, but the failure is complicated because of the multiple mixed-mode fracture occurred around the peak load. It has been noticed that an inclined shear zone may be generated during the compressive test (e.g. Strure and Ko 1978, Van Mier 1984), which may represent the structural performance if the shear zone corresponds to a joint in rock masses or a material property if the shear zone is formed by micro-cracks generated under loads.

In this study, specimens with oblique weak layers are used in order to avoid uncontrollable fracture modes in the compressive test. The primary aim of the present study is to study the damage accumulation and shear strain-softening behaviour within the pre-determined weak layer and its influence on the compressive and shear failure of the sample. The obvious advantages of such a test are: firstly, the micro-cracking zone is pre-determined so that monitoring of damage accumulation is possible, and secondly, the mixed-mode fracture and macro-crack formation can be readily and systematically controlled by varying the angle, strength and thickness of the weak layer. Potential applications of the present test includes the determination of the Mode-II and mixed-mode strain-softening behaviours of concrete-like materials, damage accumulation under creep and other loading conditions.

2 Failure Process of Cementitious Materials

2.1 The Mode-I tensile strain-softening

The well-known tensile strain-softening described by Hillerborg (1976, 1983) can be used to postulate the failure process of a mixed-mode fracture of concrete. It is known that before the softening behaviour can be measured, damage accumulation has already occurred throughout the tensile specimen in the form of micro-cracking. The process of damage accumulation becomes more intense with the increasing load, and finally

leads to the formation of a fracture zone with concentrated micro-cracks. The formation of the fracture zone or weak layer signals the load bearing capacity ceases to increase and the strain-softening becomes to show with the increasing displacement. Therefore, the tensile strain-softening characterises the fracture behaviour of the fracture zone or weak layer generated under loads. For a tensile specimen shown below the location of the damage zone or weak layer is pre-determined, i.e. at the most narrow cross-section. With a stable strain-softening curve, the area under the curve or the fracture energy G_f becomes a meaningful measurement.

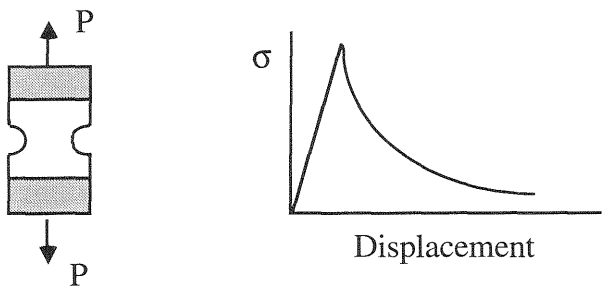

Fig. 1. Mode-I strain-softening curve of plain tensile sample

The grand success enjoyed by the fictitious crack model and tensile strain-softening signifies the importance of the fracture zone or weak layer in concrete fracture. Indeed, the well-known and equally successful smeared crack model (Bazant and Oh 1983) also points out the unique position of the fracture zone (crack band) or weak layer in concrete fracture. In fact, many fracture models including the J-integral approach (Li et al 1987) and the g_f-curve concept for the ligament effect in the fracture energy G_f (Hu 1990, Hu and Wittmann 1992) are formulated for the fracture process zone of a certain size. The fracture process zone, which can be termed as a crack band or weak layer, is an inherent characteristic of concrete fracture. It is there because of the heterogeneous characteristics of concrete. When brittle heterogeneous materials like concrete are under loads, multiple zig-zag fracture around aggregates can never be avoided.

2.2 The mixed-mode -I and -II fracture

Similar to the tensile strain-softening behaviour, a sample with a controlled fracture pattern needs to be tested to measure the Mode-II or the mixed-mode strain-softening.

The major problem of normal compressive tests with plain un-notched concrete samples is that the fracture patterns cannot be easily controlled to allow the Mode-II shear fracture to be studied within a

crack band. Therefore, mortar specimens with oblique weak layers are used in this study so that the fracture modes can be tailored systematically. Because the micro-cracking zone is pre-determined, monitoring of damage accumulation becomes an easy task. The influence of the Mode-II shear failure on the fracture of the specimens can be changed according to the angle of the weak layer θ, thickness t and strength determined by the water/cement (W/C) ratio, and sand/cement (S/C) ratio.

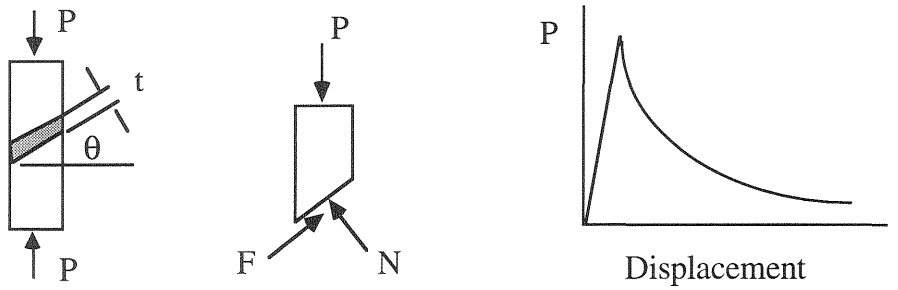

Fig. 2. Mixed-mode softening curve of sample with oblique weak layer

As illustrated in Fig. 2, a stable strain-softening curve containing the influence of the Mode-II shear failure may be obtained if fracture is confined within the weak layer. Let σ_C be the compressive stress applied. Then the shear stress τ_θ within the weak layer is given by:

$$\tau_\theta = \sigma_C \cdot \sin\theta \cdot \cos\theta \qquad (1)$$

as the shear force $F = P \bullet \sin\theta$. For a given compressive stress the maximum shear stress is obtained when $\theta = 45°$, i.e. $\tau_{max} = 0.5 \bullet \sigma_C$. It indicates the shear-strain softening should be measured around 45°. Let w be the displacement along the shear plane, δ_S be the vertical displacement of the specimen due to the sliding displacement w within the weak layer and δ_C be the vertical displacement due to the uniform compression. Then the shear strain softening function ($\tau_\theta - w$) can be derived from the load-displacement (P - δ) curve, i.e.

$$\tau_\theta = \frac{P}{A} \cdot \sin\theta \cdot \cos\theta$$
$$w = \frac{\delta_s}{\sin\theta} = \frac{\delta - \delta_c}{\sin\theta} = \frac{1}{\sin\theta} \cdot \left(\delta - \frac{L}{A} \cdot \frac{P}{E} \right) \qquad (2)$$

where A is the cross-section area perpendicular to the load P, L is the original length, E is the Young's modulus and the total displacement $\delta = \delta_S + \delta_C$. Note that if the residual displacement $\delta_r = \delta - (L/A)(P_{max}/E) \neq 0$ at the peak load P_{max}, w in equation (2) should be reduced by $\delta_r/\sin\theta$. This is because δ_r before the peak load is primarily due to the damage irrelevant to the shear strain-softening.

3 Specimen Preparation

The normal Portland cement and sand of 1 mm in diameter were used to prepare the test samples of 50 x 50 x 200 mm. The difference between the bulk material and the weak layer was controlled by the W/C and S/C ratios. The W/C and S/C ratios for the bulk mortar material were 0.4 and 1.5. Two weak layer materials were considered: material (A) with the W/C and S/C ratios of 0.7 and 3.0, and material (B) with the W/C and S/C ratios of 0.8 and 3.5. Obviously, material B is weaker than material A.

The weak layer angles were set at 0°, 10°, 20°, 30°, 45° and 50°. Note that the angle 45° for the maximum shear stress influence had been included. Three weak layer thicknesses were selected, they were 5, 10 and 15 mm. Considering the sand diameter is only 1 mm, they should be sufficiently thick to contain the shear fracture process zone.

A steel mould had been custom-made to facilitate the specimen casting. The bulk specimens were cast first while the weak layer spaces were occupied by steel plates. After about one hour, the plates were removed and the weak layers were cast. A day later the specimens were removed from the mould and cured in water for four-weeks. Compressive tests were performed immediately after the specimens were removed from the water tank. The compressive loading rate was controlled by the cross-head speed of an Instron machine, set at 0.5 mm/min.

4 Results and Discussion

4.1 Influence of weak layer on compressive failure

A diverse spectrum of failure after the peak loads has been observed ranging from stable, quasi-stable to unstable fracture. Obviously, many factors such as the test machine stiffness, displacement/loading rate, and the strength, thickness and angle of the weak layer decide the failure patterns. A quasi-stable load-displacement (P-δ) curve obtained with a specimen of material B with a weak layer of 10 mm thick and 30° angle is shown in Fig. 3. A stable load-displacement curve obtained with a

specimen, again material B, with a weak layer of 5 mm thick and 45° angle is shown in Fig. 4.

Under the experimental conditions set up arbitrarily for the sake of convenience, most specimens fractured catastrophically after the peak loads were reached. A few typical fractured specimens are shown in Figs. 5 to 10 so that the influence of various weak layers on the fracture modes and the P-δ curve behaviour can be compared and studied.

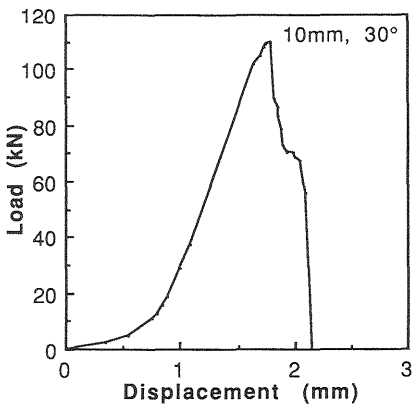

Fig. 3. P-δ curve of specimen, weak layer: mater. B, 10 mm, 30°

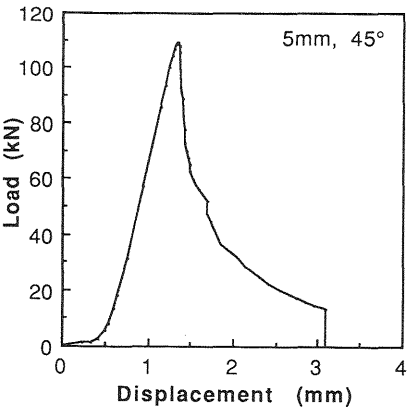

Fig. 4. P-δ curve of specimen, weak layer: mater. B, 5 mm, 45°

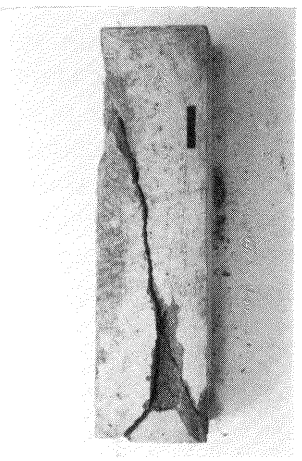

Fig. 5. Compressive failure of plain specimen (mark = 20 mm)

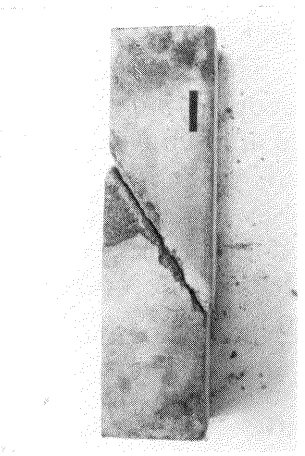

Fig. 6. Failure of specimen with weak layer: mater. B, 5 mm, 55°

Although the specimen in Fig. 5 originally did not contain a weak layer, the shear-band failure is obvious. This can be explained by the micro-cracking induced shear-band formation (e.g. Van Mier 1984). The shear-band of the specimen in Fig. 6 is pre-determined by the weak layer introduced during the specimen preparation. With the large angle

of 55° failure outside the weak layer has been virtually avoided. Under such a condition the damage accumulation before the peak load can be easily studied by the stress-strain behaviour within the weak layer, and the post- peak load P-δ curve can be readily analysed by a shear-strain softening model. Therefore, the only difference between the two specimens in Figs. 5 and 6 is that they have different strain-softening properties.

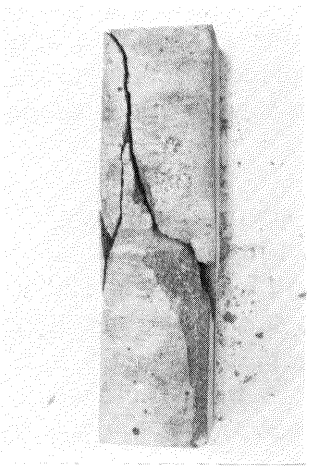

Fig. 7. Failure of specimen with weak layer: mater. B, 10 mm, 0°

Fig. 8. Failure of specimen with weak layer: mater. B, 10 mm, 20°

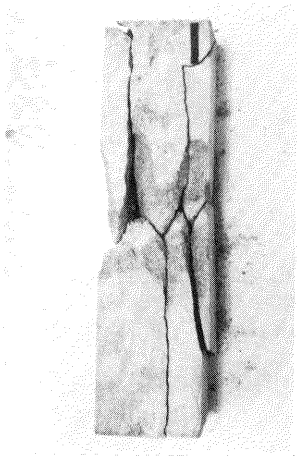

Fig. 9. Failure of specimen with weak layer: mater. B, 10 mm, 30°

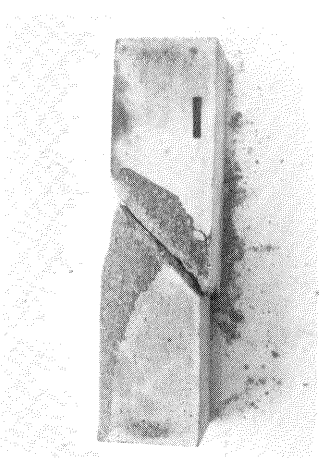

Fig. 10. Failure of specimen with weak layer: mater. B, 5 mm, 45°

Even if the angle of a weak layer is small, such as the situations in Figs. 7 and 8, the overall failure of a specimen is still influenced by the compressive/shear damage in the weak layer. The P - δ curves in Figs. 3 and 4 are corresponding to the specimens in Figs. 9 and 10. It is clear

that if failure is confined within a well-defined weak layer, the shear-strain softening can be deduced easily from the stable P - δ curve. The results in Figs. 4 and 10 appear to satisfy the requirement. In fact, the main role of the weak layers introduced in the compressive specimens is to confine failure in a well-defined region so that the failure process can be monitored and analysed. For that reason, plain concrete specimens can also be used if angled notches are cut around the specimen surfaces and they are wide and deep enough to contain the fracture process zone. The only difference between the two methods is that one approach emphasises the influence of an existing weak plane on concrete fracture, and the other considers the formation of such a weak plane or fracture zone.

4.2 Strength measurements and shear strain-softening

The compressive strengths of specimens with various weak layers (material B) have been measured and shown in Figs. 11 and 12. Results of material A specimens are similar except the strength values are higher because of smaller W/C and S/C ratios. Compared to the 5 mm thick weak layer specimens, the strengths of the 15 mm thick weak layer specimens are less sensitive to the weak layer angle, but the overall strength has been reduced.

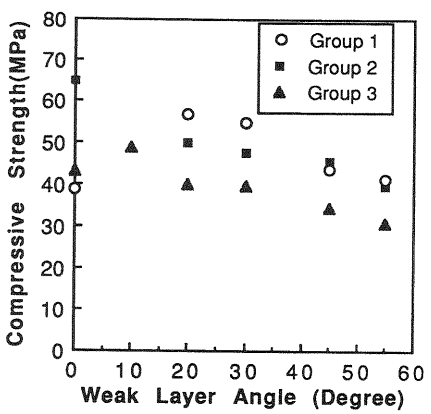

Fig. 11. Influence of weak layer angle on compressive strength (mater. B, 5 mm)

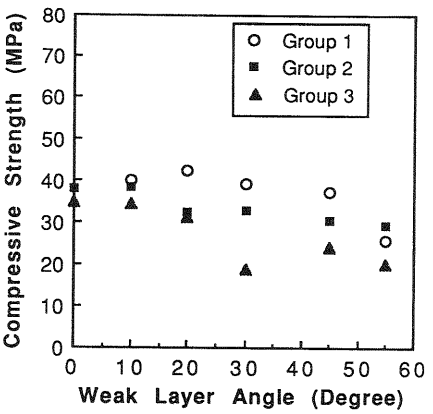

Fig. 12. Influence of weak layer angle on compressive strength (mater. B, 15 mm)

Equation (2) with the modification of the residual displacement δ_r has been used to determine the shear strain-softening shown in Fig. 13 from the P - δ curve in Fig. 4. Similar to the Mode-I strain softening, the fracture energy $G_{f\text{-}\theta}$ can be defined by the area under $\tau_\theta - w$ curve. From Fig. 13 it is obtained that $G_{f\text{-}\theta}$ = 29 kN/m compared to 30 kN/m determined by the ratio of the area under the P - δ curve over the shear

plane area A/sinθ. This value is much higher than the fracture energy G_f of the Mode-I tensile fracture possibly because of the combination of compression and shear influence.

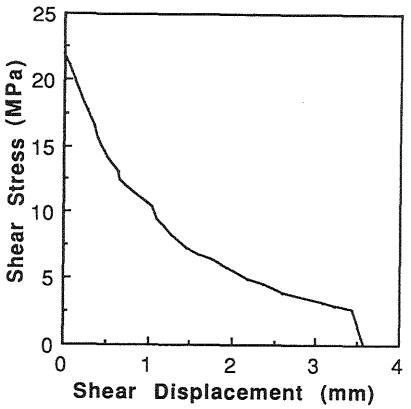

Fig. 13. Shear strain softening (τ_θ – w): mater. B, 5 mm, 45°

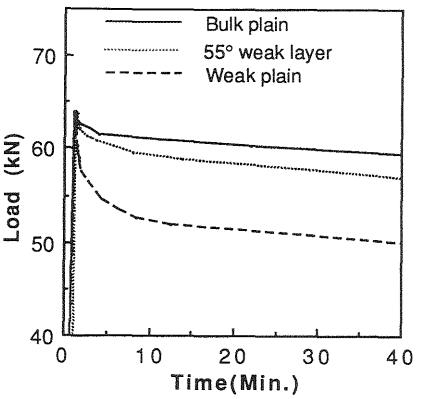

Fig. 14. Stress relaxation in plain, plain weak, and weak layer mater. B, 5 mm, 55°

The stress relaxation curves under a constant displacement are shown in Fig. 14. The behaviour of the specimen with a 55° weak layer indicates a strong influence of the weak layer. Therefore, creep within a shear band and other long-term properties can be readily monitored and studied with the weak layer specimens.

5 Concluding Remarks

Compressive fracture of mortar specimens with controlled weak layers has been studied. It is shown that with the test set-up the shear strain-softening can be deduced from the mixed-mode fracture, and the long-term properties such as creep within the weak layers can be studied. It is also realised that similar tests can be performed with plain concrete specimens so long as inclined notches which are sufficiently deep and wide are grooved.

Reference

Barr, B., Hughes, T., Khalifa, S. and Yacoub-Tokatly, A. (1989) A comparative study of geometries used to investigate the fracture behaviour of materials under mixed mode loading, in **Fracture of**

Concrete and Rock: recent development, (eds S.P. Shah, S.E. Swartz, B. Barr), Elsevier, London, 448-457.

Bazant, Z.P. and Oh, B.H. (1983) Crack band theory for fracture of concrete, **Mat. and Struct.**, 16, 155-177.

Hillerborg, A. (1983) Analysis of one single crack, in **Fracture Mechanics of Concrete**, (ed F.H. Wittmann), Elsevier, Amsterdam, 223-249.

Hillerborg, A., Modeer, M. and Petersson, P.E. (1976) Analysis of crack formation and crack growth in concrete by means of fracture mechanics and finite elements, **Cement and Concrete Research**, 6, 773-782.

Hu, X.Z. (1990) **Fracture Process Zone and Strain-Softening in Cementitious Materials**, Building Materials Report No. 1, Institute for Building Materials, Swiss Federal Institute of Technology, Zurich, Switzerland.

Hu, X.Z. and Wittmann, F.H. (1992) Fracture energy and fracture process zone, **Mat. and Struct.**, 25, 319-326.

Jenq, Y.S. and Shah, S.P. (1989) On the fundamental issues of mixed mode crack propagation in concrete, in **Fracture of Concrete and Rock: recent development**, (eds S.P. Shah, S.E. Swartz, B. Barr), Elsevier, London, 27-38.

Li, V.C., Chan, C.M. and Leung, C.K.Y. (1987) Experimental determination of the tension-softening curve in cementitious composites, **Cement and Concrete Research**, 17 (3), 441-452.

Luong, M.P. (1989) Fracture behaviour of concrete and rock under Mode-II and Mode-III shear loading, in **Fracture of Concrete and Rock: recent development**, (eds S.P. Shah, S.E. Swartz, B. Barr), Elsevier, London, 18- 26.

Sture, S. and Ko, H.Y. (1978) Strain-softening of brittle geologic materials, **Int. J. Num. Anal. Methods in Geo. Mech.**, 2, 237-253.

Van Mier, J.G.M. (1984) **Strain-Softening of Concrete under Multiaxial Loading Conditions**, Ph.D Thesis, Delft University of Technology, Netherlands.